Sesquiterpenes and oxygenated sesquiterpenes dominate the VOC (C₅-C₂₀) emissions of downy birches

Heidi Hellén[1], Arnaud P. Praplan[1], Toni Tykkä[1], Aku Helin[1], Simon Schallhart[1], Piia P. Schiestl-Aalto[2,3,4], Jaana Bäck[2,3], Hannele Hakola[1]

[1]Finnish Meteorological Institute, P.O. Box 503, 00101 Helsinki, Finland
[2]Institute for Atmospheric and Earth System Research / Forest Sciences
[3]Faculty of Agriculture and Forestry, University of Helsinki, Finland
[4]Department of Forest Ecology and Management, SLU, 901 83 Umeå, Sweden

Correspondence to: Heidi Hellén (heidi.hellen@fmi.fi)

Abstract. Biogenic volatile organic compounds (BVOCs) emitted by the forests are known to have strong impacts in the atmosphere. However, lots of missing reactivity is found especially, in the forest air. Therefore better characterization of sources and identification/quantification of unknown reactive compounds is needed. While isoprene and monoterpene (MT) emissions of boreal needle trees have been studied quite intensively, there is much less knowledge on the emissions of boreal deciduous trees and emissions of larger terpenes and oxygenated volatile organic compounds (OVOCs). Here we quantified the downy birch (*Betula pubescens)* leaf emissions of terpenes, oxygenated terpenes and green leaf volatiles (GLVs) at the SMEAR II boreal forest site using in situ gas chromatographs with mass spectrometers.

Sesquiterpenes (SQTs) and oxygenated sesquiterpenes (OSQTs) were the main emitted compounds. Mean emission rates of SQTs and OSQTs were significantly higher in early growing season (510 and 650 ng g_{dw}^{-1} h^{-1}, respectively) compared to its main (40 and 130 ng g_{dw}^{-1} h^{-1}, respectively) and late (14 and 46 ng g_{dw}^{-1} h^{-1}, respectively) periods , indicating that early leaf growth is a strong source of these compounds. The emissions had a very clear diurnal variation with afternoon maxima being on average 4 to 8 times higher than seasonal means for SQTs and OSQTs, respectively. β-Caryophyllene and β-farnesene were the main SQTs emitted. The main emitted OSQTs were tentatively identified as 14-hydroxy-β-caryophyllene acetate (M 262 g/mol) and 6-hydroxy-β-caryophyllene (M 220 g/mol). Over the whole growing season, the total MT emissions were only 24 and 17% of the total SQT and OSQT emissions, respectively. A stressed tree growing in a pot was also studied and high emissions α-farnesene and an unidentified SQT were detected together with high emissions of GLVs. Due to the relatively low volatility and the high reactivity of SQTs and OSQTs, downy birch emissions are expected to have strong impacts on atmospheric chemistry, especially on secondary organic aerosol (SOA) production.

1 Introduction

In addition to light oxygenated volatile organic compounds (OVOCs, e.g. methanol, acetone, acetaldehyde) and isoprene, monoterpenes (MTs) and sesquiterpenes (SQTs) are the major biogenic volatile organic compounds (BVOCs) emitted from the boreal forest. Both terpene groups exhibit many structural isomers, with a large range of reactivity. They influence chemical communication of plants and insects, the oxidation capacity of air and particle formation and growth. BVOC emissions are known to be highly dependent on temperature and light (Guenther et al. 2012), but also other abiotic stress factors such as frost, drought, radiation and exposure to oxidants such as ozone (Vickers et al. 2009, Loreto and Schnizler 2010, Bourtsoukidis et al. 2012 and 2014b) may have strong impacts on the emissions. In addition, biotic stress factors such as herbivore/pathogen outbreaks can initiate or alter VOC emissions (Pinto-Zevallos et al. 2013, Joutsensaari et al. 2015, Faiola and Taipale 2020).

Several studies have shown that there is a lot of unknown hydroxyl radical (OH) reactivity in the air especially in boreal forests (Yang et al., 2016). For example, in a forest in Finland isoprene, MTs, SQTs and other known reactive compounds (e.g. CO, CH_4, NO_x, O_3, NMHCs, C_1-C_6 aldehydes and C_2-C_6 organic acids) are only able to explain less than 50% of the measured total OH reactivity (Nölscher et al., 2012, Praplan et al., 2019). This missing reactivity has been suggested to originate from either unknown emitted compounds or atmospheric oxidation products of VOCs. A recent study (Praplan et al. 2019) showed that currently known oxidation products are able to explain only a minor fraction ($< 4.5\%$) of the missing reactivity in the air of boreal forest. A large fractions of missing reactivity have been found directly in the emissions of main boreal tree species (Nölcher et al. 2013, Praplan et al., 2020). To explain the missing reactivity, we need to identify the unknown compounds causing it.

Although isoprene and MTs have been studied quite intensively in boreal areas (e.g. Hakola et al., 2001, 2006, 2017; Hellén et al. 2006, 2018, Mäki et al. 2019; Kesselmeier et al., 1999; Rinne et al., 2007, 2009; Ruuskanen et al., 2007; Tarvainen et al., 2005) and there are also studies on sesquiterpenes (Bourtsoukidis et al., 2014; Hakola et al., 2001, 2006, 2017, Mäki et al. 2017, Hellén et al., 2018), knowledge on the emissions of BVOCs other than terpenes is very limited. Emissions of light OVOCs like methanol, acetone and acetaldehyde have been characterized (e.g. Mäki et al. 2019, Aalto et al. 2014, Bourtsoukidis et al. 2014a, Schallhart et al. 2018), but there is very little information on the emissions of higher OVOCs. König et al. (1995) found significant oxygenated hydrocarbon emissions from Silver birch (*Betula pendula*), Hakola et al. (2017) found emissions of C_5-C_{10} aldehydes from Norway spruces and Wildt et al. (2003) detected stress induced emissions of C_5-C_{10} aldehydes from 6 different plant species in their laboratory experiments. To our knowledge there are no publications on birch emission rates of oxygenated sesquiterpenes (OSQTs). Zang et al. (1999) detected them in the head space of downy birch branches and Isidorov et al. (2019) in the head space of collected birch buds. They are also known to be a major component in the essential oils of birches (Dimirce et al. 2000, Klike et al. 2004). Earlier they have been detected in the emissions of desert and Mediterranean shrubs and some trees growing in the warmer vegetation zones (Matsunaga et al. 2009, Yaman et al. 2015 and Yanez-Serrano et al. 2018). Due to their larger size and lower vapour pressure these OSQTs are expected to be highly reactive

and to have higher comparative secondary organic aerosols yields than isoprene and MTs and therefore even low emissions may have strong impacts in the atmosphere.

85   There are many studies on BVOC emissions of the main coniferous trees in boreal forests, but the data on deciduous trees is more limited (Guenther et al., 2012). Birches are common deciduous broadleaved trees in northern and central Europe and in Asia, being most abundant in the boreal zone of northern Europe, where they can co-dominate or dominate in late-successional forests (Beck et al. 2016). Downy birch *(Betula pubescens)* occur naturally throughout most of Europe up to central Siberia, growing further north in Europe than any other tree species (Beck et al. 2016).

90   Downy and silver birch emissions in natural environment have been studied by Hakola et al. (1998, 2001), and König et al. (1995) and mountain birch (subspecies of downy birch) emissions by Ahlberg (2011) and Haanpanala et al. (2009). They have found highly variable emissions of both MTs and SQTs.

Here we set up to study the downy birch emissions of terpenes, OVOCs and green leaf volatiles (GLVs) at the SMEAR

95   II boreal forest site using in situ gas chromatographs with mass spectrometers (GC-MSs).

2   Methods

100   **2.1 Studied trees**

Downy birch (*Betula pubescens* Ehrh*.*) emission measurements were conducted at the SMEAR II station (Station for Measuring Forest Ecosystem–Atmosphere Relations; 61°51'N, 24°18'E; 181 a.s.l.) in Hyytiälä, southern Finland (Hari and Kulmala, 2005). In 2017, a young downy birch (height of about 2 m) was planted in a 10-liter pot with a mixture of mineral soil and fertilized growth peat and placed next to the measurement container. The seedling received normal

105   rainwater and in drier periods it was watered. In 2019, a downy birch (height ~4 m) growing naturally next to the container was measured.

Measurements were conducted at different stages of the leaf development (Table 1). In 2017 during the early growing season measurement period (24–28/5/2017) leaves of the downy birch were growing fast (Fig. 1). During the main

110   growing season (samples taken 21–28/6/2017 and 13–19/7/2017) leaves were fully grown and some leaf damages were detected. Visible signs of senescence of the leaves started during the late growing season (samples taken 23-28/8/2017). Because the birch studied in 2017 was growing in a pot, it suffering of the artificial stress due to dry zero air used for the flushing the measurement chamber and possibly occasional problems in watering the pot.

115   In 2019, when the naturally growing tree was measured, growth of the leaves started a bit earlier than in 2017. In 2019, samples were taken already during the bud break period, when the leaves did not grow fast yet, between 7 and 15 May ('bud'). After that the fast leaf growth started and continued over the early growing season (samples taken during the period 18/5–7/6/2019, 'early'). During the main growing season (samples taken during the periods 18/6–5/7/2019 and 21–27/7/2019, 'main') leaves were fully grown and in the end of the late growing season (samples taken during the

120   period 10–23/8/2019, 'late') senescence of leaves was starting. The two first measurements ('bud' and 'early') were

conducted from the same branch, and in the following periods two new branches were measured, so that altogether three branches were used in the measurements in both years

Table 1. Sampling schedule showing the measurement periods during each stage (bud/early/main/late) of the growing season.

Year	Bud	Early	Main	Late
2017	n.a.	24/–28/5	21–28/6	23–28/8
			13–19/7	
2019	7–15/5	18/5–7/6	18/6–5/7	10–23/8
			21–27/7	
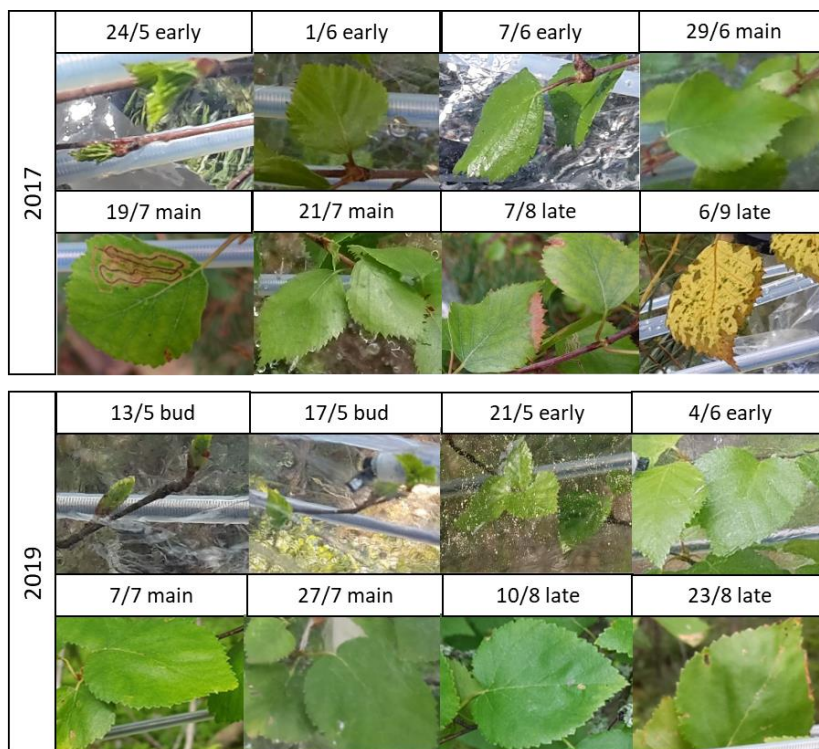
Figure 1: The measured leaves over the growing seasons in 2017 and 2019

2.2 Branch chamber measurements

2.2.1 Measurement set up

For the measurements, the downy birch branches were placed in a FEP enclosure (~6L cylinder) and the emission rates were measured using a steady state flow-through technique (Hakola et al. 2017). In 2017 the measured branch was enclosed for 1 to 2 weeks at the time. In 2019 the same branch was enclosed before the bud brake and during the early growing season measurements between 6/5-7/6, and after that for 1-2 weeks at the time. The FEP cover was removed after each measurement period and put back in place again at least 30 min before the next measurement, allowing the branch to experience ambient conditions in between. After closing the chamber, the sample collection started immediately, but results from the first samples were discarded. A zero air generator (HPZA-7000, Parker Hannifin Corporation) was used to produce the air flushed through the chamber (the flow rate was recorded continuously, and it was approximately $2.9 – 5.3$ L min^{-1} and $6.0 – 7.1$ L min^{-1} in 2017 and 2019, respectively). Due to the high reactivity and short atmospheric lifetimes of the studied compounds, their ambient air concentrations are much lower than concentrations in our emission chamber. Therefore, we do not expect any artificial emissions by using zero air. However, in 2017, due to dry zero air, relative humidity of the air in the branch chamber was very low (mean 32 ± 9 %). In addition, during that year the birch was growing in a pot and even though it was watered regularly, it is possible that there were occasional short drought episodes. In 2019, the in-going zero air was humidified with ultrapure water, and the mean relative humidity of the air in the chamber was 66 ± 19 %. The relative humidity (RH) and the temperature in the enclosure were recorded with a thermistor (Philips KTY 80/110, Royal Philips Electronics, Amsterdam, Netherlands) and the photosynthetically active radiation (PAR) was measured with a quantum sensor (LI-190SZ, LI-COR, Biosciences, Lincoln, USA) placed on top of the enclosure. The main flow going to the instruments was approximately at flow rate of 0.8 L min^{-1} and $1.5 – 4.7$ L/min in 2017 and in 2019, respectively. The main sampling line was a FEP tubing (ca. 5 m length, i.d. 1/8″) in 2017. In 2019, the main sampling line was a heated FEP tubing (ca. 10 m length, i.d. 1/8″) in all other periods except on $25 – 27/7$, during which the sampling line was an unheated FEP tubing (ca. 13.5 m length, 3/8" i.d). For most target compounds losses in these sampling lines and chamber are expected to be negligible as demonstrated by the acceptable recoveries observed in the laboratory tests (Helin et al., 2020; Hellén et al., 2012), and since high flow rates were used. Even though the only OSQT studied (caryophyllene oxide) had also an acceptable recovery (>80%), some losses of higher molecular weight compounds (i.e. diterpenes) in the chamber were detected and therefore it is possible that there are some losses of higher OSQTs also in the current study and our OSQT emission rates are underestimated.

In order to determine the emission rates per leaf biomass, the measured branches were cut, dried at +60ºC and the leaves were weighted.

2.2.2 Temperature effect

The temperature inside the branch chamber is known to increase more than ambient temperatures in sunny conditions (e.g. Ortega and Helmig, 2008; Rinnan et al., 2014). Higher temperature is expected to induce more emissions. The flow through the chamber during the measurements was maintained at 3 to 7 L min^{-1} to keep the leaf surface temperature close to the chamber air temperature. In 2019, it was always > 6 L min^{-1}. However, the temperature of the leaves is also known to be higher than ambient air temperature in sunny conditions. To characterize this we measured surface temperature of the leaves during the emission measurements using an infrared thermometer (IRT 206) in July/August 2019. Measured leaves were from the branches next to our branch chamber.

2.3 GC-MS analysis

Emissions of MTs, SQTs, oxygenated MTs (OMTs), oxygenated SQTs (OSQTs), isoprene, C_5-C_{10} aldehydes (ALD) and green leaf volatiles (GLVs) were measured from branch chambers with two in situ thermal desorption-gas chromatograph-mass spectrometers (TD-GC-MSs). These measurements enabled molecular level identification and quantification of compounds having vapour pressure corresponding to the vapour pressure of alkanes having 5 to 20 carbon atoms. With the method it was not possible to quantitatively measure compounds with <5 carbon atoms (e.g. methanol, acetone, acetaldehyde), which are also known to be emitted by the vegetation (Mäki et al. 2019, Aalto et al. 2014, Bourtsoukidis et al. 2014a, Schallhart et al. 2018). However, due to high volatility of these compounds, they are not expected to have strong impacts on secondary organic aerosol formation in the atmosphere.

In 2017 and in 2019, one instrument (GC-MS1) was used for the measurements of individual MTs, SQTs, isoprene and OMTs (1,8-cineol, linalool, α-terpineol). Additionally in 2017, ALDs, and in 2019 OSQTs and *cis*-3-hexen-1-ol were measured with this instrument. Measured compounds are listed in Table A1 in the appendix A. VOCs were collected in the cold trap (Tenax TA 60-80/ Carbopack B 60-80 and Tenax TA 60-80 in 2017 and 2019, respectively) of the thermal desorption unit (TurboMatrix 350, Perkin-Elmer) connected to a gas chromatograph (Clarus 680, Perkin-Elmer) coupled to a mass spectrometer (Clarus SQ 8 T, Perkin-Elmer). To remove humidity, the cold trap was kept at 25°C during sampling. Between the 2017 and 2019 measurements, the thermal desorption unit was modified to enable the measurements of less volatile compounds, namely OSQTs. Stainless steel lines inside the online box of the TD unit were changed to FEP tubing and an empty sorbent tube used in the TD inlet line was changed to glass coated stainless steel tube. The optimization of the method is described in Helin et al. (2020). These TD unit changes and the use of a GC column with a lower film thickness enabled the measurement of OSQTs. A HP-5 column (60 m, id. 0.25 mm, film thickness 1 µm, from Agilent Technologies) and a Elite-5MS column (60 m, id. 0.25 mm, film thickness 0.25 µm, from Perkin-Elmer) were used for separation in 2017 and 2019, respectively. To calibrate compounds other than isoprene, standards were injected as methanol solutions into sorbent tubes (Tenax TA 60-80/Carbpack B 60-80) and the tubes were thermally desorbed and analyzed as samples. Five-point calibration curves were used. To calibrate isoprene, a gas standard from National Physical Laboratories (UK) was used instead of a methanol solution. Blank values measured by sampling an empty cuvette were subtracted from the results. The blank value was negligible for terpenes but varied between 3 to 7 ng g_{dw}^{-1} h^{-1} for aldehydes measured in 2017. SQTs (α-farnesene and SQT1-7), OSQTs (OSQT1-9) and MTs (β-ocimene and sabinene) lacking authentic standards were tentatively identified based on the comparison of the mass spectra and retention indexes (RIs) with NIST mass spectral library (NIST/EPA/NIH Mass Spectral Library, version 2.0). These tentatively identified compounds were quantified using response factors of calibrated compounds having the closest RI and mass spectra resemblance. Regarding OSQTs, an authentic standard was available only for caryophyllene oxide. 30-minute samples at a flow rate of 40 mL min^{-1} were collected every hour or every other hour. The total number of samples were 407 and 1102 in 2017 and 2019, respectively. Typical chromatograms of a calibration standard, emission sample and blank sample can be found from the appendix B.

In 2017, an additional instrument (GC-MS2) was used for the measurements of GLVs. Measured compounds are listed in Table A2 in the appendix A. Samples were analyzed in situ with a thermal desorption unit (Unity 2 + Air Server 2, Markes International LTD) connected to a gas chromatograph (Agilent 7890A, Agilent Technologies) and a mass spectrometer (Agilent 5975C, Agilent Technologies). A polyethylene glycol column, the 30 m DB-WAXetr (J&W 122-7332, Agilent Technologies, Santa Clara, CA, USA, i.d. 0.25mm, film thickness 0.25 μm) was used for the separation. Samples were taken every other hour. The sampling time was 60 min and the flow rate was 40 mL min^{-1}. The method has been described in Hellén et al. (2017 and 2018).

2.4 Defining the growth of the leaves

Daily growth rate of the leaves, G^i, was modelled with the CASSIA model (Schiestl-Aalto et al., 2015) where the daily growth is driven by environmental variables, mainly daily mean temperature. CASSIA has previously been parameterized for Scots pine at the SMEAR II station, and the model has been shown to successfully predict the growth of different tree organs (Schiestl-Aalto et al., 2015). Here, the model was parameterized for birch with leaf area growth measured from photographs taken three times per week during summers 2015 and 2016 and specific leaf mass measured from the growing leaves during the same dates. These measurements started immediately after bud braea, so the model describes the leaf growth from the beginning. The correlation between the modeled and measured leaf growth was good. Furthermore, the parameter defining the timing of bud break was fitted to the observed bud break of our measurement branches. The mass of growing leaves on day d is then $W_d = \sum_{i=1}^{d} G^i$ and the relative leaf mass on day d is $W_d^r = W_d/W_e$ where W_e is the leaf mass on the last day of the measurement period.

2.5 Sampling of additional trees

To screen the birch individuals for their potential chemodiversity, additional samples from 1–5 m tall downy and silver birches growing naturally close to the measurement container were taken in 2019. Branches were closed into a FEP-bags and 5-minute samples with a flow of approx. 200 ml min^{-1}, with the exact flow logged at the beginning and the end of sampling, were collected from the head space of the birch branches into the Tenax TA(60-80)-Carbopack B(60-80) sorbent tubes. The sample tubes were analysed later in the laboratory using a similar method as for the online samples (offline sorbent tube analysis, e.g. Helin et al. (2020)). These measurements were semi-quantitative and they were only used for qualitative analysis of terpene emission patterns. Since the concentrations in the FEP-bags were clearly higher than the ambient air concentrations, no subtraction of the initial concentration level was conducted.

2.6 Calculation of emission potentials

It is well-known that monoterpene emissions from coniferous boreal forests have an exponential temperature dependence (Guenther et al. 2012). The Guenther algorithm was used for calculating the emission potentials at 30°C (Guenther et al., 1993):

$$E_{30} = \frac{E}{\exp(\beta(T - T_S))}$$

where E_{30} is the standard emission potential at 30 °C (ng g_{dw}^{-1} h^{-1}), T is the chamber temperature (°C), T_S is the standard temperature (30 °C) and β is the temperature sensitivity (°C^{-1}) of emissions, which was solved simultaneously with E_{30}. In addition to seasonal mean emission potentials, daily mean emission potentials (E_{30}) were calculated for 2019 for all days with more than half of the measurements available. To test if some of the emissions had delayed temperature effect emissions were also correlated with 2 hour time lag of temperature.

BVOC emissions may also be correlated with the level of irradiation, thus the emission potentials for light and temperature dependent emission (E_{CTxCL}) were also calculated with an algorithm developed by Guenther et al. (1993 and 1995). The temperature inside the chamber and the PAR measured on top of the chamber were used for these calculations. The standard emission potential can be obtained by linearly fitting the emission rates to the light and temperature activity factors (CTxCL) of the emission algorithm. Emission potentials ($E_{CT x CL}$) were defined at Ts 30°C and PAR 1000 µmol m^{-2} s^{-1}. Unfortunately, the PAR sensor was not working/installed properly during the bud break season in 2019, thus the E_{CTxCL} could not be calculated for this period. In addition, the average PAR received by leaves inside the chamber is expected to be less than measured above the chamber influencing the light and temperature dependent emission calculations.

3 Results and discussion

3.1 Emission rates of BVOCs

The highest total BVOC emissions from downy birch leaves were detected during the early growing season (Fig. 2 and Appendix A Table A1), i.e. from leaves that were still growing both for naturally growing tree and for the tree growing in a pot in 2019 and 2017, respectively. High early growing season emissions indicate that these emissions are related to bud break/early growth of leaves, which has previously been shown, e.g., in Scots pine foliage (Aalto et al 2014). The SQTs and OSQTs were clearly the main compound groups emitted. On average total SQT emissions were 5 and 4 times higher than total MT emissions in 2017 and 2019, respectively. OSQT emissions (measured only in 2019) were 5.8 times higher than MT emissions. Emissions of C_4-C_{10} aldehydes (measured only in 2017) were as low or lower than MT emissions. In 2017, when GC-MS2 was used for measuring GLVs, high emission rates were observed simultaneously with leaf damages. As discussed in section 3.1.5 higher than natural emissions may have been induced inside our chamber, especially in sunny conditions, due to elevated chamber temperature compared to ambient conditions.
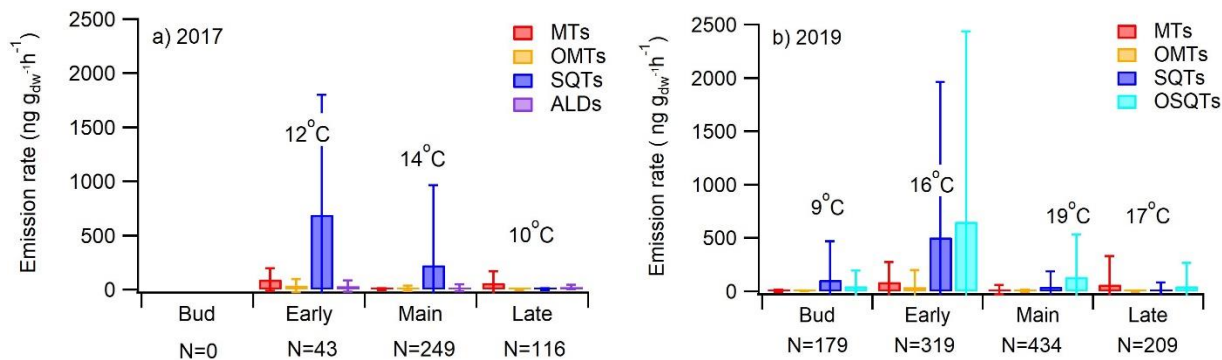
Figure 2: Season (bud break, early, main, late) mean± standard deviation emission rates of different VOC groups and mean chamber temperature in a) 2017 (tree growing in a pot) and b) 2019 (naturally growing tree). N is the number of samples. ALD=C_4-C_{10} aldehydes measured only in 2017.

Emissions were peaking in the afternoon, coinciding with the highest temperature and PAR, and were very low during the night (Fig 3). During the early growing season, when emissions were the highest, also some nighttime emissions were detected, indicating that the emissions are not just light dependent, but there are also emissions from storage pools in downy birch. Due to clearly higher emissions in the afternoon and short lifetime of the terpenes, they are expected to have major effect on atmospheric chemistry especially during that time of the day.
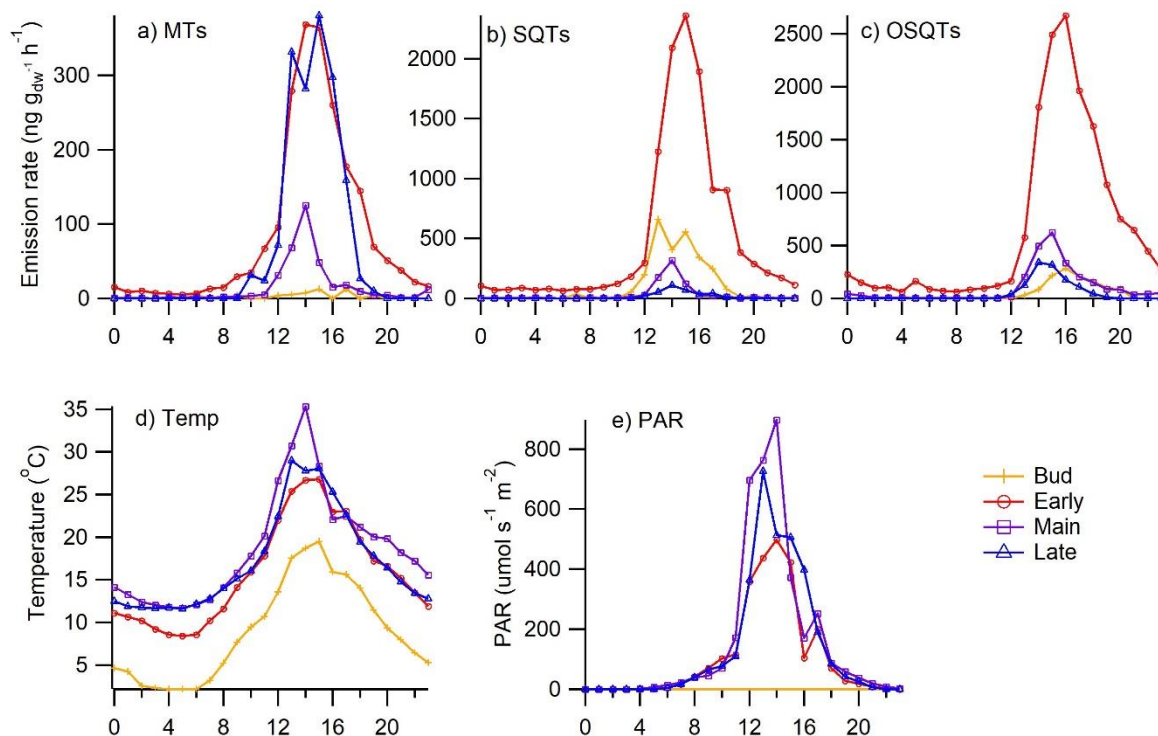
Figure 3: Mean seasonal diurnal variation of emission rates of a) MTs, b) SQTs and c) OSQTs and d) chamber temperature and e) PAR during different seasons in 2019. During bud break PAR was not measured.

310

3.1.1 Monoterpenoid emissions

MT emission rates were the highest during the early growing season, decreased during the main growing season and peaked again at the end (Fig. 2 and 3), which was comparable to a previous study from downy birch (e.g. Hakola et al 2001). Of the MTs, α-pinene, β-pinene, limonene and sabinene were the most abundant compounds except during the last two days of the measurements in August in 2019, when β-ocimene emissions had the major contribution (Fig. 4a). This could indicate that ocimene emissions are related to the senescence of the leaves. Our finding supports the previous observations, e.g. the ones from Vuorinen et al. (2005) where (E)-β-ocimene and (Z)-ocimene were main compounds emitted by the Silver birches in August. In addition to late growing season emissions, Vuorinen et al. (2007) found strong herbivore induced emissions of ocimenes from Silver birches.

320

Linalool, one of the OMTs, had the highest emissions during the early growing season (Table A1 in the appendix A and Fig. 4b). For the birch growing in the pot in 2017, linalool had also relatively high emissions in June and July while it was not detected at all at the end of the growing season in August. For naturally growing birch in 2019, linalool was detected only during the early growing season, similarly as reported by Hakola et al. (2001) who detected high linalool emissions from downy birch also in early growing season. However, linalool emission is also known to be induced by stress in Norway spruce (Petterson, 2007; Blande et al., 2009). The potential relationship of linalool with birch stress emissions is addressed later in Section 3.4.

3.1.2 SQT emissions

330 SQT emissions from the downy birch were clearly higher than MT emissions, except in the end of the growing season (Fig. 2). Mean emission rates in 2017 (measured tree in the pot) were significantly higher during the early growing season (692 ng g_{dw}^{-1} h^{-1}) than in its main or late periods (226 ng g_{dw}^{-1} h^{-1} and 5 ng g_{dw}^{-1} h^{-1} respectively). Similarly, in 2019, when the naturally growing tree was measured, mean SQT emission rates in early season were 505 ng g_{dw}^{-1} h^{-1} while in in main or late season they were only 41 and 14 ng g_{dw}^{-1} h^{-1}, respectively. Afternoon emissions were clearly higher than these seasonal means being on average 2360, 320 and 110 ng g_{dw}^{-1} h^{-1} for early, main and late growing seasons, respectively (Fig. 3). High SQT emissions have been observed also in earlier studies of downy birch (Hakola et al., 2001, Räsänen et al., 2017) and mountain birch (*Betula pubescens* ssp. czerepanovii), which is a subspecies of downy birch (Haapanala et al., 2009).

340 In 2017, when the measured tree was growing in a pot, individual SQTs emission pattern changed dramatically over the growing season (Fig. 4c). In May, when the leaves were growing, β-caryophyllene had the highest contribution, while in the end of the growing season, it was not detected at all. α-Farnesene had very low emissions in May, while during the other seasons, it was the major SQT detected. In July 2017, emissions of an unidentified SQT (SQT7) were even higher than emissions of α-farnesene, while in May and June it was negligible. Since the birch in 2017 was likely

suffering from leaf damage, drought and high chamber temperatures, it is possible that SQT7 and α-farnesene are stress related emissions (see Section 3.4). Hakola et al. (2001) found high emissions of β-caryophyllene from all downy birches, but α-farnesene was emitted only from young trees. In 2019, when naturally growing tree was used, α-farnesene and SQT7 were not detected and β-caryophyllene, β-farnesene and α-humulene were the main emitted SQTs. As in 2017 contributions of β-caryophyllene and α-humulene were the highest during early growing season, which indicates that their emissions are related to early growth of the leaves. Later in 2019, β-farnesene was dominating.

3.1.3 OSQT emissions

OSQTs were measured only in 2019. High emissions were measured especially during the early growing season (Fig. 2b). Seasonal mean emission rates for OSQT (651, 134 and 46 ng g_{dw}^{-1} h^{-1} during early, main and late growing seasons) were a bit higher than for SQTs. Afternoon emissions were clearly higher than these seasonal means being on average 2670, 620 and 340 ng g_{dw}^{-1} h^{-1} for early, main and late growing seasons, respectively (Fig. 3). In total, 9 different OSQTs were detected and the ratios of different OSQTs remained fairly constant over the growing season (Fig. 4d). The only OSQT identified and quantified with an authentic standard was caryophyllene oxide. However, it was <9% of the total measured OSQT mass. In headspace studies of the downy birch leaves by Zang et al. (1999), caryophyllene oxide was also the only OSQT identified and its contribution to the total OSQT mass was 11%. Isidorov et al. (2019) found several different OSQTs in the headspace of downy birch buds and of the OSQTs, 14-hydroxy-β-caryophyllene acetate (M 262 g mol^{-1}) had the highest contribution. 14-Hydroxy-β-caryophyllene acetate has also been shown to be the major component of essential oils of birch species native to Turkey (Demirci et al. 2000) and of essential oils of downy and mountain birch buds (Klika et al. 2004). Our mass spectra and retention indexes indicate that OSQT9, the major compound found in our studies, is 14-hydroxy-β-caryophyllene acetate. The second highest OSQT3 was tentatively identified as 6-hydroxy-β-caryophyllene (M 220 g mol^{-1}). It was also the second highest contributor of OSQTs in the headspace samples of downy birch buds (Isidorov et al. 2019).

3.1.4 Other BVOC emissions

Isoprene emissions were very low (season means < 0.4 ng g_{dw}^{-1} h^{-1}) both in 2017 and 2019. The seasonal mean emission rates of ALDs, measured only in 2017, were 33, 16 and 23 ng g_{dw}^{-1} h^{-1} during early, main and late seasons, respectively. Variation of the emission ratios of aldehydes was high (Table A1 in the appendix A). Decanal was the most significant C_4-C_{10} aldehyde during the leaf growth, but after that hexanal and nonanal emissions became more important. Hexanal, nonanal and decanal were also major C_4-C_{10} aldehydes emitted by a Norway spruce (Hakola et al. 2017). Possanzini et al. (2000) and Bowman et al. (2003) have observed emissions of these larger aldehydes (e.g. heptanal, octanal and nonanal) when ozone attacks the fatty acids on leaf or needle surfaces. However, in our system ozone-free zero air was used.

In 2017 an additional in situ GC-MS2 was used for measuring emissions of GLVs. The time of the measurements did not always overlap with GC-MS1 measurements of terpenes and aldehydes and therefore they cannot unfortunately be directly compared. GLV measurements were conducted during early (26/5 – 7/6/2017), main (21/6 – 19/7/2017) and late (23/8 – 25/8/2017) growing seasons. *cis*-3-Hexen-1-ol and *cis*-3-hexenylacetate were the most significant GLVs. Their emissions were high especially in July (mean 475 ng g_{dw}^{-1} h^{-1}, max 8500 ng g_{dw}^{-1} h^{-1}), when also some leaf

damages were detected. GLVs containing six carbon atoms are emitted directly by plants often as a result of physical damage (Fall, 1999; Hakola et al., 2001). These emissions could also be drought induced since, in 2017, the measured birch was suffering from it. In 2019, the only GLV measured with GC-MS1 was *cis*-3-hexenol, but emissions remained below the detection limit ($<$30 ng g_{dw}^{-1} h^{-1}).

3.1.5 The branch chamber temperature

Due to elevated branch chamber temperature compared to ambient conditions, higher than natural emissions may have been induced inside our chamber, especially in sunny conditions. However, this effect is not as high as the difference between ambient air and chamber temperature would indicate since also temperature of the close by leaves increased clearly higher than ambient temperatures in sunny conditions (Table 2). Results show that the surface temperature of the leaves next to the chamber in direct sun was on average 8°C higher than ambient air temperature while chamber temperature was 14 °C higher. In partly cloudy conditions difference between leaf surface and ambient air was 7 °C and between chamber and ambient air 10 °C. Without direct sun leaf surface temperatures were 1.4 °C lower than the ambient temperature and chamber temperature was very close to the ambient temperature with the mean difference being only +0.4 °C.

Table 2. Mean ambient air, downy birch leaf next to the chamber and branch chamber temperatures measured at the same time in the end of July and early August in 2019 in sunny, partly cloudy and cloudy conditions.

Temperature (°C)	Ambient	Leaf surface (ambient)	Chamber
Sunny	23.7	32.0	37.8
Partly cloudy	26.0	32.7	35.7
Cloudy	25.3	23.7	25.6
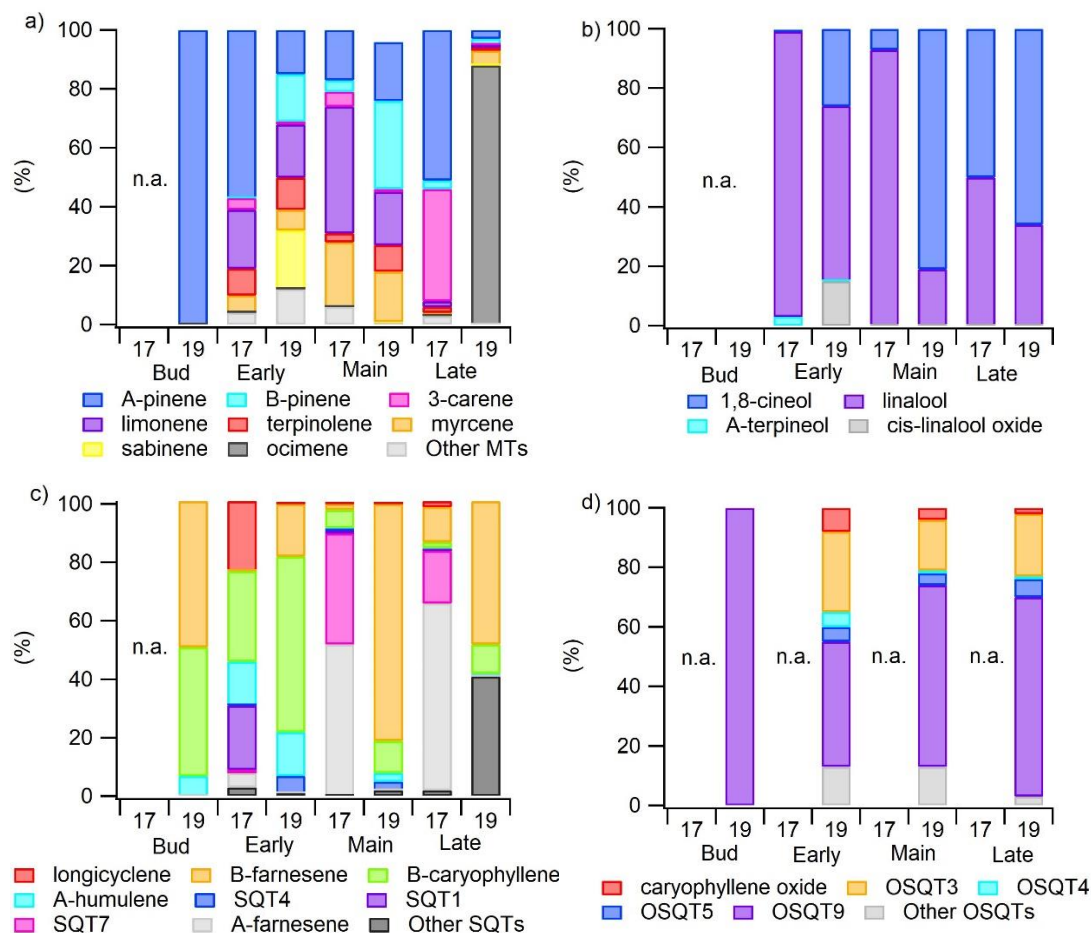
410 Figure 4: Emission ratios of individual a) MTs b) OMTs, c) SQTs and d) OSQTs during early, main and late growing seasons in 2017 (17) and 2019 (19).

3.2 Variation of the emission ratios between the trees

415 Different chemotypes have been found for Scots pine, one with high α-pinene and the other with high 3Δ-carene emissions (Bäck et al. 2012). To study the variability of compounds emitted by different birch trees, ratios of BVOCs were measured from the headspace of 13 additional birch branches growing close to the main trees in 2019. Of the measured birches, eight were downy birches, one a silver birch and four were either downy or silver birches. Isoprene had very low contribution in the emissions of all measured trees over the whole growing season (Fig. 5). As for the

420 main trees measured with the in situ TD-GC-MS, in the beginning of growing season in May, SQTs and OSQTs were clearly the most important compounds for most of the trees. Later, contribution of MTs increased and in the end of growing season, the contributions of SQTs and OSQTs were very low. However, there were clear differences between the trees and for instance the fraction of MTs varied in May between 3% and 31% (Fig. 5). In their studies of three different downy birches Hakola et al. (2001) found also highly varying emission ratios of terpenes. For one of their

425 trees MTs and an OMT (linalool) were clearly the most significant compounds emitted while for the other two trees SQTs had major contribution. Such inherent diversity in secondary metabolism is often seen in both downy birch and silver birch: Stark et al (2008) reported qualitative, but not quantitative, latitude-associated gradient in the foliar

flavonoids in downy birch, Makhnev et al. (2012) found genetic differences in triterpene content of silver birch leaf extracts, and Deepak et al. (2017) associated the genotype with differences in triterpenoids and alcyl coumarates in the surface waxes of silver birch.
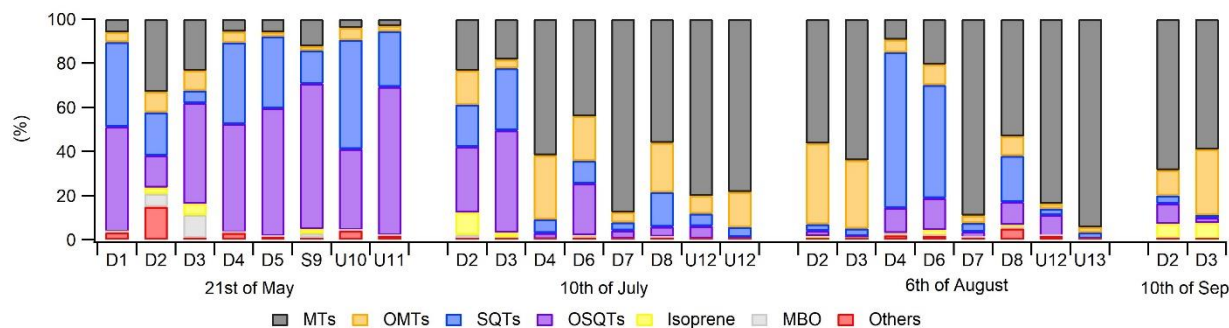
Figure 5: Ratios of BVOC groups in the headspace of different tree branches measured over the growing season in 2019. Numbering indicates different trees, and none were the same as the ones described in Section 2.1. Of the trees D1-D8 were identified as downy birches, S9 was a silver birch and U10-13 were either downy or silver birches.

Ratios of individual terpenes in the head space of the branches can be found from Figure C1 in the appendix C. As for the main trees measured with the in situ TD-GC-MS, of the MTs α-pinene, β-pinene, limonene and sabinene had the highest ratios. However, limonene was detected mainly during the early growing season. In the studies of Isidorov et al. (2019), limonene was the major MT detected in the head space analysis of downy birch buds. Of the OMTs, linalool and one unidentified OMT, had the largest contribution in the emissions of all trees during early growing season, but during the other seasons 1,8-cineol was clearly the major OMT. β-Caryophyllene and β-farnesene were the major SQTs emitted throughout the growing season. One unidentified SQT (SQT4) had occasionally also a strong contribution. β-Caryophyllene and β-farnesene dominated also the emissions of main trees in 2019 (Fig. 4c). Ten different OSQTs were detected in the emissions of studied trees, OSQT9 (tentatively identified as 14-hydroxy-β-caryophyllene acetate) being the major emitted compound. Caryophyllene oxide was detected only in the early growing season, while contribution of OSQT4 increased after that. OSQT9 (tentatively identified as 14-hydroxy-β-caryophyllene acetate) had also major contribution in the emissions from the main tree in 2019 (Fig. 4d).

These results indicate that the tree-to-tree variability in emission patterns seems significant, but still rather small compared to the seasonal variability (growing season). Even though emission ratios vary a lot over the growing season, there seems to be fairly systematic trend in it (i.e. relatively dominant SQT and OSQT ratios during early growing season and increasing contribution of MTS and OMTs during the main and late growing season). However, there can be some birches with very different emission ratios. We were unable to identify clear chemotypes as for the Scots Pine by Bäck et al. (2012).

3.3 Temperature and light dependence of the emissions

Temperature is a significant factor controlling the biogenic emissions (Guenther et al. 2012). However, at least MT emissions from birch leaves are also correlating with light (Hakola et al. 2001, Rinne et al., 2009, Ghirardo et al., 2010). In their $^{13}CO_2$ labelling studies, Ghirardo et al. (2010) found, that all MTs emitted from the silver birch (*Betula pendula*) were from the *de novo* biosynthesis. In darkening experiments of downy birch branches by Hakola et al. (2001), most of the MT emissions declined to values below detection limit very fast after covering the branch, while the darkening effect on SQTs was very low. This indicates that while MTs mainly originate from *de novo* emissions, SQT emissions are likely mostly temperature dependent and coming mainly from the storage pools. However, as shown in Fig. 3, some emissions of MTs were detected also during night especially during high emissions in the early growing season (PAR=0.0 µmol m^{-2} s^{-1}, MT emission 10 ng m^{-2} h^{-1}) and therefore they are expected to have some temperature dependent emissions from storage pools as well. We defined both temperature (E_{30}) and light and temperature (E_{CTxCL}) dependent emission potentials at 30°C and at 1000 µmol m^{-2} h^{-1} for our downy birch emissions (Table 3). Uncertainties in PAR received by the leaves due to PAR measurements conducted above the chamber possibly influenced E_{CTxCL} calculations and with better PAR measurements R^2 values for the *de novo* emissions could be higher.

Table 3. Exponential correlation of emission rates (ng g_{dw}^{-1} h^{-1}) with temperature, linear correlation with light and temperature activation factor (CTxCL) and emission potentials during bud break in 2019 and during early, main and late growing seasons in 2017 and 2019. E_{30}=temperature dependent emission potential at 30°C, E_{CTxCL}= light and temperature dependent emission potential at 30°C and at PAR 1000 µmol m^{-2} s^{-1}, β=temperature sensitivity, R^2=correlation coefficient, a=intercept of the linear fitting of light and temperature dependence curve E=b·CTxCL+a, where E is the emission. Values with correlation coefficient R^2<0.3 have been italicized and colored grey. Low correlations can be mostly explained by the emission rates detected being very close to or below detection limits and therefore having high uncertainty.

2017	MTs			SQTs			ALDs		
	E_{30}	β	R^2	E_{30}	β	R^2	E_{30}	β	R^2
$\underline{T_{30}}$	ng g_{dw}^{-1} h^{-1}	°C^{-1}		ng g_{dw}^{-1} h^{-1}	°C^{-1}		ng g_{dw}^{-1} h^{-1}	°C^{-1}	
Early	319	0.06	0.43	5640	0.14	0.58	350	0.15	0.61
Main	*4*	*0.03*	*0.04*	500	0.13	0.46	39	0.10	0.36
Late	*36*	*0.06*	*0.01*	*10*	*0.02*	*0.00*	4260*	0.30	0.73
$\underline{CTxCL}$	E_{CTxCL}	a	R^2	E_{CTxCL}	a	R^2	E_{CTxCL}	a	R^2
	ng g_{dw}^{-1} h^{-1}			ng g_{dw}^{-1} h^{-1}			ng g_{dw}^{-1} h^{-1}		
Early	*270*	*124*	*0.07*	5100	494	0.61	240	37	0.57
Main	*5*	*3.8*	*0.02*	1540	50	0.40	80	12	0.52
Late	*74*	*-240*	*0.01*	*7*	*11*	*0.00*	480	14	0.57

2019	MTs			SQTs			OSQTs		
	E_{30}	β	R^2	E_{30}	β	R^2	E_{30}	β	R^2
$\underline{T_{30}}$	ng g_{dw}^{-1} h^{-1}	°C^{-1}		ng g_{dw}^{-1} h^{-1}	°C^{-1}		ng g_{dw}^{-1} h^{-1}	°C^{-1}	

Bud	44	0.01	0.14	1601	0.10	0.56	543	0.03	0.11
Early	187	0.15	0.70	770	0.13	0.68	948	0.11	0.41
Main	32	0.14	0.77	74	0.14	0.57	340	0.07	0.33
Late	63	0.06	0.07	85	0.08	0.26	416	0.09	0.31
CTxCL	E_{CTxCL} ng g_{dw}^{-1} h^{-1}	a	R^2	E_{CTxCL} ng g_{dw}^{-1} h^{-1}	a	R^2	E_{CTxCL} ng g_{dw}^{-1} h^{-1}	a	R^2
Bud	n.a.	n.a.	n.a.	n.a.	n.a.	n.a.	n.a.	n.a.	n.a.
Early	370	20	0.62	1590	108	0.33	2317	1858	0.15
Main	76	2	0.72	189	7	0.55	429	253	0.11
Late	405	99	0.13	149	101	0.03	572	315	0.08

*Due to emission rates close to the detection limits and low chamber temperature (<18.7°C) upscaling to the 30°C can give unrealistic value. Linear fitting gives as high R^2 value, but then the emission potential is only 124 ng g_{dw}^{-1} h^{-1}.

Emission potentials showed a very high variation between the seasons as well as within the season (Table 3 and Figure 6). The highest potentials were measured during the bud break and early growing season. Even if the bud break emission potentials are high especially for the SQTs, real emissions are still low since the leaf mass is very low (<10% of the mass of fully grown leaves) during that period. After the early growing season emission potentials decreased considerably in June and July. During the late growing season emissions of SQTs and OSQTs were as low as during the main growing season, but for MTs relatively high emissions were detected during the last two days of measurements in 2019.

Of the OSQTs the only compound detected during the bud break period was OSQT9 (14-hydroxy-β-caryophyllene acetate). Correlation with temperature during that time was low (R^2=0.11, Table 3). If we use a 2h time lag for temperature, correlation was clearly higher (R^2=0.39) and emission potential of OSQT9 was 615 ng g_{dw}^{-1} h^{-1}. However, even with this high emission potential, emissions are expected to be low due to the low biomass of the leaves during bud break. Also, during the early growing season correlation with temperature was better while using the temperature measured two hours earlier. It is possibly explained by delayed temperature response of these less volatile compounds in the leaves and losses and re-evaporation of them on the inlet and branch chamber walls. In our earlier tests we have detected some losses of higher molecular weight compounds into our chamber and particularly in the instrument (Helin et al. 2020). Based on this and due the fact that OSQT9 had higher molecular weight, more oxygen atoms and more double bonds than caryophyllene oxide, it is possible that the real emissions may be even higher than those observed here.

For the ALDs, very high emission potential (4260 ng g_{dw}^{-1} h^{-1}) was observed during the late growing season in August 2017 (Table 3). Even though the linear fit of the temperature dependence resulted in high R^2 value, the emission potential was only 124 ng g_{dw}^{-1} h^{-1} when using the linear fitting (R^2=0.73) for the temperature dependence curve. Chamber temperature during these late growing season measurements was always <18.7 °C and most of the measured

emission rates were very close to the detection limits. The highest measured emission rate of aldehydes was 103 ng g_{dw}^{-1} h^{-1}. Therefore, the upscaling of these results to 30 °C may be unrealistic.

GLVs, measured only in 2017, were slightly correlated with temperature during the main (R^2=0.41) and late (R^2=0.31) growing seasons, but temperature was not the main factor controlling their emission. GLV emissions coincided with leaf damages and were potentially stress induced (Section 3.4).
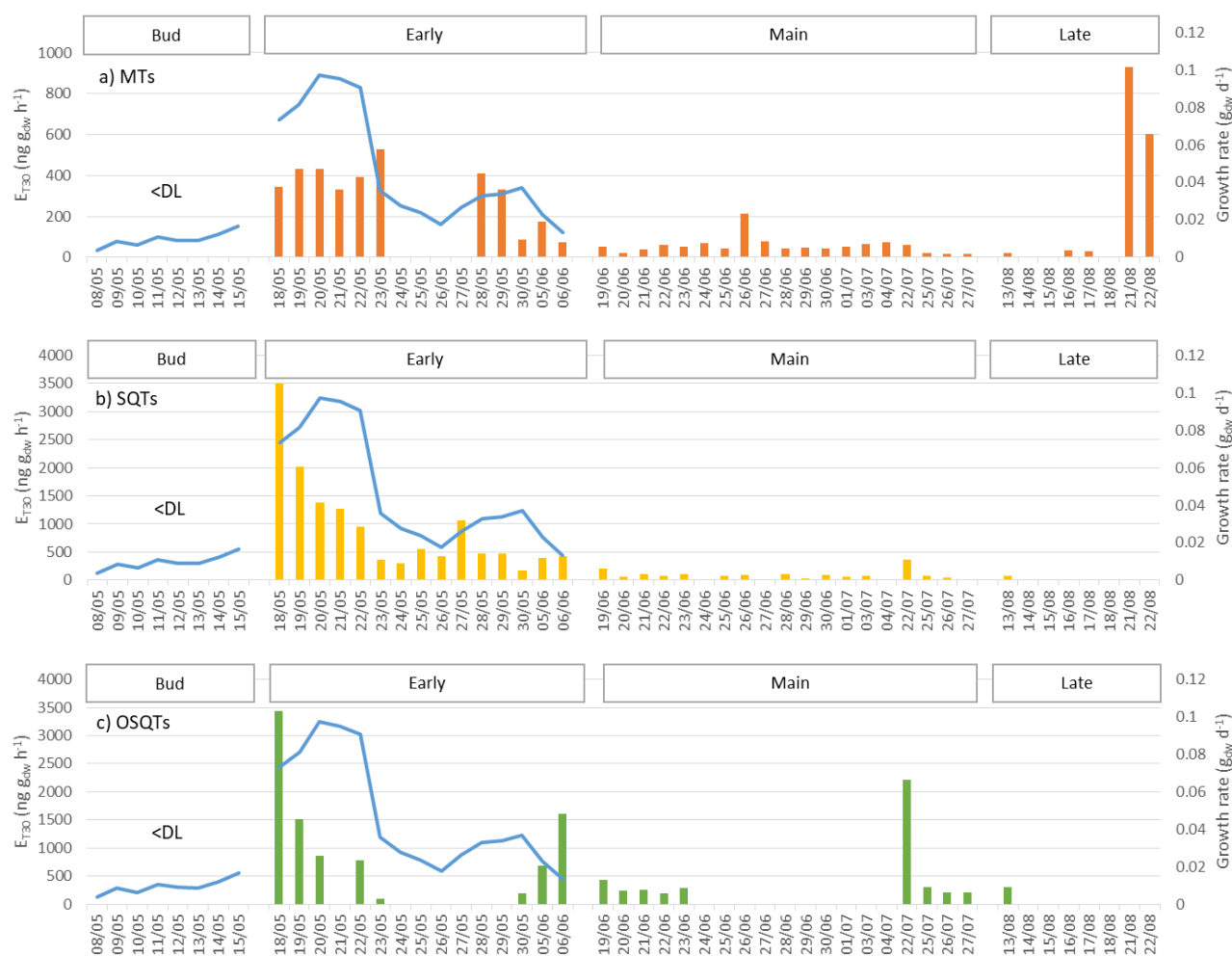
Figure 6: Daily mean emission potentials at 30°C ($E_{30,day}$) of a) MTs, b) SQTs and c) OSQTs (bars) during bud break, early, main and late growing seasons in 2019 and modeled growth rate of leaves (g_{dw} day^{-1}) of the measured branch (blue line). During the budbreak period emission rates were often below detection limits and there were too few points for calculation of daily emission potentials. Emission potentials of days with low temperature correlation (R^2<0.3) were omitted. Potentials were calculated only for the days with more than 12h measured.

Daily mean emission potentials ($E_{30,day}$) were calculated for 2019 for all days with more than half of the measurements available. During the early growing season, the mean daily correlation coefficients (R^2) between the emission rates and temperature were 0.84, 0.86 and 0.51 for MTs, SQTs and OSQTs, respectively. Even though short term and diurnal

variations of the emissions were explained well by the temperature, the development of the buds and growth of leaves had a very strong effect on the emission potentials (Fig. 6). The highest daily emission potentials were measured during the highest growth rate and a decrease followed with the decrease of the growth rate of the leaves. This suggests that there could be storage pools of these compounds in the buds, which are released after the bud break. Isidorov et al. (2019) detected huge amounts of different VOCs, including SQTs and OSQTs, in the headspace of downy birch buds. For OSQTs additional peak in the emission potentials was observed on 22 July.

For MTs, the highest daily mean emission potentials were detected during the last two days of measurements in August. As mentioned before, this was due to the high emissions of one MT, tentatively identified as β-ocimene. It is possible that ocimene emissions are related to the senescence of leaves, but also herbivore induced ocimene emissions have been detected (Vuorinen et al. 2007).

Emission potentials found in earlier studies are listed in Table 4. Even though at least MT emissions from birches are known to be also light dependent (Hakola et al. 2001, Rinne et al., 2009, Ghirardo et al., 2010), most studies report emission rates normalized to only by temperature. Therefore, only temperature (E_{30}) normalized emission potentials are compared here. Emission potentials reported vary over 3 orders of magnitude, the lowest MT emission potential of downy birch being only 5 ng g_{dw} h^{-1} and the highest 5000 ng g_{dw} h^{-1}. For downy birch SQT emissions the lowest reported emission potential was 17 ng g_{dw} h^{-1} and the highest 6900 ng g_{dw} h^{-1}. It is noteworthy that most of the earlier studies are only from short periods or laboratory conditions, and do not report the seasonal variation of the emission potentials. As shown here for MTs, SQTs and OSQTs and by Hakola et al. (2001) for MTs, seasonal variation is very high and this could explain at least part of the differences in results from literature. Variation in MT and SQT emission potentials between birch species is up to several magnitudes when comparisons have been made in similar conditions.

Table 4. Comparison of emission potentials normalized to temperature 30°C (E_{30}, ng g_{dw}^{-1} h^{-1}). Emission potentials with very low correlation ($R^2<0.3$) has been omitted from this study data. ETS=effective temperature sum describing the state of the growing season.

Birch type	Season	MTs (E_{30})	SQTs (E_{30})	OSQTs (E_{30})	Refs.
Downy	Early	-	5110	-	This study, 2017
	Early	190	770	950	This study, 2019
	ETS<80	1470	-	-	Hakola et al. (2001), tree 1
	Main	-	500	-	This study (2017), stress
	Main	32	74	340	This study (2019)
	80<ETS<400	720	-	-	Hakola et al. (2001), tree 1
	80<ETS<400	310	-	-	Hakola et al. (2001), tree 2
	80<ETS<400	310	-	-	Hakola et al. (2001), tree 3
	Late	5	-	-	This study, 2017
	Late	-	-	420	This study, 2019

	ETS>400	5490	-	-	Hakola et al. (2001), tree 1
	ETS>400	1710	-	-	Hakola et al. (2001), tree 2
	ETS>400	170	-	-	Hakola et al. (2001), tree 3
	Summer	-	310	-	Hakola et al. (2001), tree 1
	Summer	-	6940	-	Hakola et al. (2001), tree 2
	Summer	-	810	-	Hakola et al. (2001), tree 3
	unspecified	3000	2000	-	Karl et al. (2009)
	laboratory	5-10	17-31	-	Räsänen et al. (2017)[a]
Silver	ETS<80	3630	-	-	Hakola et al. (2001)
	80<ETS<400	680	-	-	Hakola et al. (2001)
	ETS>400	7710	-	-	Hakola et al. (2001)
	unspecified	3000	2000	-	Karl et al. (2009)
	laboratory	23-188	41-190	-	Räsänen et al. (2017)[a]
Mountain	Main	31	35	--	Ahlberg et al. (2011)
	Main	5300	6500	-	Haapanala et al. (2009)

[a] Converted using foliar density 240 g m^{-2} obtained from Karl et al. (2009)

3.4 The effect of stress on the emissions

Stress induced emission were detected in 2017 when the measured birch was growing in a pot possibly due to dry zero air flushed into the chamber and too low watering of the pot. In 2019, the used zero air was humidified and the tree was growing naturally. The low relative humidity (mean RH 31%) in the chamber in 2017, may have caused stomatal closure due to water (?) vapour pressure deficit. In 2019 RH in the chamber was clearly higher (mean RH 63 %). The effect of stress in 2017 was confirmed by the strong emissions of GLVs which are known to be stress related compounds.

In July 2017 the branch was visibly suffering from leaf damages (Fig. 1) and possibly effects of drought. During that time very high emissions of two GLVs, *cis*-3-hexen-1-ol and *cis*-2-hexenylacetate, were detected (max. 1500 and 6900 ng g$_{dw}$$^{-1}$ h^{-1}, respectively). In July simultaneously with GLV emissions, high emissions of two SQTs (SQT7 and α-farnesene) were detected as well (max. 4700 and 1800 ng g$_{dw}$$^{-1}$ h^{-1}, respectively). However, emissions of GLVs were the highest in the afternoon on 18 July, while for the SQTs the highest emissions were measured on 16 July. Relatively high α-farnesene emissions were detected also in the end of June together with emission of *cis*-3-hexen-1-ol and *cis*-2-hexenylacetate, but SQT7 remained below detection limits during that time. Also some linalool emissions (up to 23 ng g$_{dw}$$^{-1}$ h^{-1}) were detected during these stress periods. In 2019, emissions of all these compounds remained very low or below detection limits.

While SQT7 emission potentials during the stress period in July 2017 had very high correlation with the chamber temperature (R^2=0.95, β=0.17 ^{O}C^{-1}, E$_{30}$=268 ng g$_{dw}$$^{-1}$ h^{-1}), and also α-farnesene showed some temperature dependence

($R^2=0.53$, $\beta=0.11$ $^\circ$C^{-1}, $E_{30}=209$ ng g_{dw}^{-1} h^{-1}), *cis*-3-hexen-1-ol and *cis*-2-hexenylacetate emissions did not follow the changes in temperature or light ($R^2=0.21$ and 0.31, respectively) but were the highest on 18 July when the temperature was lower than the previous days.

Results indicate that even though *cis*-3-hexen-1-ol, *cis*-2-hexenylacetate, α-farnesene, linalool and SQT7 emissions seemed to be stress related, mechanisms behind their emissions may be different. Earlier studies have found that GLVs are emitted by plants as a result of physical damage (Fall, 1999; Hakola et al., 2001) and α-farnesene emissions are known to be highly sensitive to the biotic stress (Kännaste et al. 2008, Faiola and Taipale, 2020).

3.5 Atmospheric implications of the emissions

In their emission inventory for the boreal ecosystem in Finland, Tarvainen et al. (2007) estimated that MTs are the major terpene group emitted (84% total flux) and that SQTs are mostly only emitted in July and August, with downy and silver birches as the largest contributor. The share of SQTs on total terpene flux was estimated to be 7%. Taking into account our results with high emission potentials of SQTs already in May and June, the importance of SQTs would be much higher. The oxidation products of VOCs play a key role in secondary aerosol (SOA) formation, especially in forested areas (Ehn et al., 2014; Kulmala et al., 2013) and SQTs produce higher comparative aerosol yields than isoprene and abundant MTs, and consequently may contribute significantly to SOA formation (Griffin et al. 1999; Lee et al., 2006, Frosch et al. 2013). Oxidation products of SQTs have very high cloud condensation activity and therefore these birch emissions potentially have high impacts also on cloud formation (Be et al., 2017). OSQT emission potentials were even higher than for SQTs in our study. With their higher molecular weights and lower volatilities they could have even higher SOA yields than SQTs, but to our knowledge, this has not been studied yet. Due to very high reaction rates of SQTs and possibly OSQTs with O_3 and hydroxyl radicals (OH), their effects on local oxidation capacity is also expected to be strong and should warrant further investigation.

4 Conclusions

Even though isoprene is the main BVOC emitted globally (Gunther et al. 1995), it is clear that downy birches do not contribute to its emissions. The main VOC groups emitted by the downy birches were SQTs and OSQTs especially in the beginning of the boreal summer in May and early June. Downy birches were also a source of MTs, ALDs and GLVs. However, emission ratios of the studied VOCs were highly variable over the growing season.

The highest BVOC emissions were detected during the early growing season indicating that early growth of leaves is a strong source of these compounds. Of the SQTs, especially β-caryophyllene and α-humulene emissions were clearly related to early growth season, whereas, later, their emissions were very low or below detection limits. Of the OSQTs, two compounds tentatively identified as 14-hydroxy-β-caryophyllene acetate and 6-hydroxy-β-caryophyllene had a major contribution over the whole growing season with emissions being clearly the highest during the early growing season. In 2017, leaf damages and stress possibly related to drought and high chamber temperature was found to induce emissions of GLVs (*cis*-3-hexen-1-ol and *cis*-2-hexenylacetate), linalool, α-farnesene and an unidentified SQT. The emissions of BVOCs were peaking in the afternoon together with temperature and PAR and were very low during the night.

Earlier studies have shown that MT emissions of downy birches are mainly light dependent, and our results mainly agree with this although some nighttime emissions were also detected. However, our results indicated that emissions of SQTs and OSQTs from downy birch foliage are mostly temperature dependent. The highest seasonal emission potentials of MTs, SQTs and OSQTs were observed during the bud break and early growing season. Daily emission potentials were the highest during the fastest leaf growth period and a decrease in emission potentials followed the decrease of the growth rate of the leaves. This indicates that there could be storage pools of these compounds in the buds, which are released after the bud break. Due to high variability of the emissions over the growing season, it is clear that estimating birch emissions should take into account the seasonality of emission potentials.

The results indicate that downy birch can be a significant contributor for the relatively high SQT concentrations found in the boreal forest air (Hellén et al., 2018). These emissions may have strong effects especially on SOA formation. In addition, emissions of OSQTs are as high as SQT emissions and may have strong impacts in the atmosphere as well. SOA formation potential of downy birch emissions is expected be high especially during the early growing season due to high emissions of compounds with high SOA formation potentials (SQTs, OSQTs and limonene).

We used the dynamic enclosure technique to conduct these measurements, because we were mainly interested in the emissions of very reactive compounds and for that purpose enclosure measurements are the only option. However, this method disturbs plant somewhat, and therefore in addition to the leaf level measurements, also ecosystem scale measurements should be conducted.

Data availability. GC-MS and complementary data used in this work are available from the authors upon request (heidi.hellen@fmi.fi).

Author contributions. H. Hellén designed and conducted the VOC measurements, performed the data analysis and led the writing of the manuscript. H. Hakola supervised the study, helped designing the measurement campaign and the commented on the manuscript. S.Schallhart, T.Tykkä, A. Helin and A. Praplan conducted the VOC measurements and data analysis and commented on the manuscript. P.P. Schiestl-Aalto and J. Bäck provided the trees to measure in 2017 and data on leaf growth and wrote their description and commented on the manuscript.

Competing interests. The authors declare that they have no conflict of interest.

Acknowledgements. The research was supported by the Academy research fellow projects (Academy of Finland, project No. 275608 and No. 307797), Academy of Finland Postdoctoral Researcher Funding (323255), Academy of Finland project (No. 316151), Knut and Alice Wallenberg Foundation (no. 2015.0047) and Academy of Finland via the Center of Excellence in Atmospheric Sciences (No. 307331).

References

Aalto, J., Kolari, P., Hari, P., Kerminen, V.-M., Schiestl-Aalto, P., Aaltonen, H., Levula, J., Siivola, E., Kulmala, M., and Bäck, J.: New foliage growth is a significant, unaccounted source for volatiles in boreal evergreen forests, Biogeosciences, 11, 1331–1344, https://doi.org/10.5194/bg-11-1331-2014, 2014.

Ahlberg E.: BVOC emissions from a subarctic Mountain birch: Analysis of shortterm chamber measurements, Master degree project, Department of Earth and Ecosystem Sciences, Seminar series nr 204, Lund University, Sweden.

Be A.G., Upshur M.A., Liu P., Martin S.T., Geiger F.M. and Thompson R.J., 2017: Cloud activation potentials for atmospheric a-pinene and b-caryophyllene ozonolysis products, ACS Cent. Sci. 2017, 3, 715−725, DOI: 10.1021/acscentsci.7b00112.

Beck, P., Caudullo, G., de Rigo, D., Tinner, W., 2016. *Betula pendula, Betula pubescens* and other birches in Europe: distribution, habitat, usage and threats. In: San-Miguel-Ayanz, J., de Rigo, D., Caudullo, G., Houston Durrant, T., Mauri, A. (Eds.), *European Atlas of Forest Tree Species*. Publ. Off. EU, Luxembourg, pp. e010226+.

Blande, J. D., Turunen, K., and Holopainen, J. K.: Pine weevil feeding on Norway spruce bark has a stronger impact on needle VOC emissions than enhanced ultraviolet-B radiation, Environ. Pollut., 157, 174–180, 2009.

Bourtsoukidis, E., Bonn, B., Dittmann, A., Hakola, H., Hellén, H., and Jacobi, S.: Ozone stress as a driving force of sesquiterpene emissions: a suggested parameterisation, Biogeosciences, 9, 4337–4352, doi:10.5194/bg-9-4337-2012, 2012.

Bourtsoukidis, E., Bonn, B., and Noe, S.: On-line field measurements of BVOC emissions from Norway spruce (Picea abies) at the hemiboreal SMEAR-Estonia site under autumn conditions, Boreal Environ. Res., 19, 153–167, 2014a.

Bourtsoukidis, E., Kawaletz, H., Radacki, D., Schutz, S., Hakola, H., Hellén, H., Noe, S., Molder, I., Ammer, C., and Bonn, B.: Impact of flooding and drought conditions on the emission of volatile organic compounds of Quercus robur and Prunus serotina, Trees, 28, 193–204, 2014b.

Bowman, J. H., Barket, D. J., and Shepson, P. B.: Atmospheric chemistry of nonanal, Environ. Sci. Technol., 37, 2218–2225, 2003.

Bäck, J., Aalto, J., Henriksson, M., Hakola, H., He, Q., and Boy, M.: Chemodiversity of a Scots pine stand and implications for terpene air concentrations, Biogeosciences, 9, 689–702, doi:10.5194/bg-9-689-2012, 2012.

Deepak M., Lihavainen J., Keski-Saari S., Kontunen-Soppela S., Salojärvi J., Tenkanen A., Heimonen K., Oksanen E. and Keinänen M: Genotype- and provenance-related variation in the leaf surface secondary metabolites of silver birch. Can. J. For. Res. 48, 494–505, dx.doi.org/10.1139/cjfr-2017-0456, 2018.

Demirce B., Baser K.H.C., Özek T. and Demirci: Betulenols from Betula species, Planta Med., 66, 490-493, 2000.

Ehn, M., Thornton, J. A., Kleist, E., Sipilä, M., Junninen, H., Pullinen, I., Springer, M., Rubach, F., Tillmann, R., Lee, B., Lopez- Hilfiker, F., Andres, S., Acir, I.-H., Rissanen, M., Jokinen, T., Schobesberger, S., Kangasluoma, J., Kontkanen, J., Nieminen, T., Kurtén, T., Nielsen, L. B., Jørgensen, S., Kjaergaard, H. G., Canagaratna, M., Maso, M. D., Berndt, T., Petäjä, T., Wahner, A., Kerminen, V.-M., Kulmala, M., Worsnop, D. R., Wildt, J., and Mentel, T. F.: A large source of low-volatility secondary organic aerosol, Nature, 506, 476–479, doi:10.1038/nature13032, 2014.

Faiola C. and Taipale D.: Impact of insect herbivory on plant stress volatile emissions from trees: A synthesis of quantitative measurements and recommendations for future research. Atmospheric Environment X, 5, https://doi.org/10.1016/j.aeaoa.2019.100060, 2020.

Fall, R.: Biogenic emissions of volatile organic compounds from higher plants, in: Reactive Hydrocarbons in the Atmosphere, edited by: Hewitt, C. N., San Diego, Academic Press, 43–96, 1999.

Frosch, M.; Bilde, M.; Nenes, A.; Praplan, A. P.; Jurányi, Z.; Dommen, J.; Gysel, M.; Weingartner, E.; Baltensperger, U. CCN activity and volatility of β-caryophyllene secondary organic aerosol. Atmos. Chem. Phys. 2013, 13 (4), 2283−2297.

Ghirardo A., Koch K., Taipale R., Zimmer I. N. A., Schitzler J.-P. and Rinne J. 2010. Determination of de novo and pool emissions of terpenes from four common boreal/alpine trees by 13CO2 labelling and PTR-MS analysis. *Plant, Cell & Environment,* 33, 781-792.

Griffin, R. J., Cocker III, D. R., Flagan, R. C., and Seinfeld, J. H.: Organic aerosol formation from the oxidation of biogenic hydrocarbons, J. Geophys. Res., 104(D3), 3555–3567, 1999.

Guenther, A., Zimmerman, P. R., Harley, P. C., Monson, R. K., and Fall, R.: Isoprene and monoterpene emission rate variability: Model evaluations and sensitivity analyses, J. Geophys. Res., 98, 12 609–12 617, 1993.

Guenther, A.B., C.N. Hewitt, D. Erickson et al.: global-model of natural volatile organic-compound emissions. J. Geophys. Res.–Atmos. 100:8873–8892, 1995.

Guenther, A. B., Jiang, X., Heald, C. L., Sakulyanontvittaya, T., Duhl, T., Emmons, L. K., and Wang, X.: The Model of Emissions of Gases and Aerosols from Nature version 2.1 (MEGAN2.1): an extended and updated framework for modeling biogenic emissions, Geosci. Model Dev., 5, 1471-1492, https://doi.org/10.5194/gmd-5-1471-2012, 2012.

Haapanala S., Ekberg A., Hakola H., Tarvainen V., Rinne J., Hellén H., and Arneth A.: Mountain birch – potentially large source of sesquiterpenes into high latitude atmosphere, Biogeosciences, 6, 2709-2718, 2009.

Hakola H., Laurila T., Lindfors V., Hellén H., Gaman A., and Rinne J.: Variation of the VOC emission rates of birch species during the growing season. Boreal Environment Research, 6, 237-249, 2001.

Hakola H., Tarvainen V., Bäck J., Rinne J., Ranta H., Bonn B., and Kulmala M., 2006. Seasonal variation of mono- and sesquiterpene emission rates of Scots pine. Biogeosciences, SRef-ID: 1726-4189/bg/2006-3-93, 93-101.

Hakola, H., Tarvainen, V., Praplan, A. P., Jaars, K., Hemmilä, M., Kulmala, M., Bäck, J., and Hellén, H.: Terpenoid and carbonyl emissions from Norway spruce in Finland during the growing season, Atmos. Chem. Phys., 17, 3357-3370, doi:10.5194/acp-17-3357-2017, 2017.

Hari, P. and Kulmala, M.: Station for measuring ecosystem-atmosphere relations (SMEAR II), Boreal Environ. Res., 10, 315–322, 2005.

Helin, A., Hakola, H., & Hellén, H. (2020). Optimisation of a thermal desorption–gas chromatography–mass spectrometry method for the analysis of monoterpenes, sesquiterpenes and diterpenes. Atmospheric Measurement Techniques, 13(7), 3543-3560.

Hellén H., Hakola H., Pystynen K.-H., Rinne J. and Haapanala S., 2006. C2-C10 hydrocarbon emissions from a boreal wetland and forest floor. Biogeosciences, 3, 167-174.

Hellén, H., Schallhart, S., Praplan, A. P., Petäjä, T., and Hakola, H.: Using in situ GC-MS for analysis of C_2-C_7 volatile organic acids in ambient air of a boreal forest site, Atmos. Meas. Tech., 10, 281-289, doi:10.5194/amt-10-281-2017, 2017.

Hellén, H., Praplan, A. P., Tykkä, T., Ylivinkka, I., Vakkari, V., Bäck, J., Petäjä, T., Kulmala, M., and Hakola, H.: Long-term measurements of volatile organic compounds highlight the importance of sesquiterpenes for the atmospheric chemistry of a boreal forest, Atmos. Chem. Phys., 18, 13839-13863, https://doi.org/10.5194/acp-18-13839-2018, 2018.

Isidorov V. A., Stocki M. ab´nd Vetchinikova L.: Inheritance of specific secondary volatile metabolites in buds of white birch Betula pendula and Betula pubescens hybrids. *Trees,* 33**,** 1329-1344, 2019.

Joutsensaari, J., Yli-Pirilä, P., Korhonen, H., Arola, A., Blande, J. D., Heijari, J., Kivimäenpää, M., Mikkonen, S., Hao, L., Miettinen, P., Lyytikäinen-Saarenmaa, P., Faiola, C. L., Laaksonen, A., and Holopainen, J. K.: Biotic stress accelerates formation of climate-relevant aerosols in boreal forests, Atmos. Chem. Phys., 15, 12139–12157, doi:10.5194/acp-15-12139-2015, 2015.

Karl, M., Guenther, A., Köble, R., Leip, A., and Seufert, G.: A new European plant-specific emission inventory of biogenic volatile organic compounds for use in atmospheric transport models, Biogeosciences, 6, 1059–1087, https://doi.org/10.5194/bg-6-1059-2009, 2009.

Kesselmeier, J. and Staudt, M.: Biogenic volatile organic compounds (VOC): An overview on emission, physiology and ecology. Journal of Atmospheric Chemistry, 33, 23-88, 1999.

Klika K.D., Demirci B., Salminen J.-P., Ovcharenko V.V., Vuorela S., Baser K.H.C. and Pihlaja K.: New, Sesquiterpenoid-Type Bicyclic Compounds from the Buds of *Betula pubescens* _ Ring-Contracted Products of β-Caryophyllene? Eur. J. Org. Chem. 2627-2635 DOI: 10.1002/ejoc.200300808, 2004.

Kulmala, M., Kontkanen, J., Junninen, H., Lehtipalo, K., Manninen, H. E., Nieminen, T., Petaja, T., Sipila, M., Schobesberger, S., Rantala, P., Franchin, A., Jokinen, T., Jarvinen, E., Aijala, M., Kangasluoma, J., Hakala, J., Aalto, P. P., Paasonen, P., Mikkila,J., Vanhanen, J., Aalto, J., Hakola, H., Makkonen, U., Ruuskanen, T., Mauldin, R. L., Duplissy, J., Vehkamaki, H., Back, J., Kortelainen, A., Riipinen, I., Kurten, T., Johnston, M. V., Smith, J. N., Ehn, M., Mentel, T. F., Lehtinen, K. E. J., Laaksonen, A., Kerminen, V. M., and Worsnop, D. R.: Direct observations of atmospheric aerosol nucleation, Science, 339, 943–946, doi:10.1126/science.1227385, 2013.

König G., Brunda M, Puxbaum H., Hewitt C.N., Duckham S.C. and Rudolph J.: Relative contribution of oxygenated hydrocarbons to the total biogenic VOC emissions of selected mid-European agricultural and natural plant species, Atmospheric Environment, 29, 861-874, 1995.

Kännaste, A., Vongvanich, N., and Borg-Karlson, A.-L.: Infestation by a Nalepella species induces emissions of a – and b-farnesenes, (-)-linalool and aromatic compounds in Norway spruce clones of different susceptibility to the large pine weevil, Arthropod-Plant Inte., 2, 31–41, doi:10.1007/s11829-008-9029-4, 2008.

Lee, A.; Goldstein, A. H.; Keywood, M. D.; Gao, S.; Varutbangkul, V.; Bahreini, R.; Ng, N. L.; Flagan, R. C.; Seinfeld, J. H. Gas-phase products and secondary aerosol yields from the ozonolysis of ten different terpenes. J. Geophys. Res. 2006, 111, D07302.

Loreto, F. and Schnitzler, J.-P.: Abiotic stresses and induced BVOCs, Trends Plant Sci., 15, 154–166, 2010.

Makhnev, A.K., Degtyarev, E.S., and Migalina, S.V.: Intraspecific variality of triterpene content in the leaves of Betula pendula Roth. Contemp. Probl.. Ecol., 5(2): 179–184. doi:10.1134/S1995425512020096, 2012.

Matsunaga S.N., Guenther A., Greenberg J. P., Potosnak M., Papiez M., Hiura T., Kato S., Nishida S., Harley P and Kajii Y.: Leaf level emission measurement of sesquiterpenes and oxygenated sesquiterpenes from desrt shrubs and temperate forest trees using liquid extraction technique. Geochemicla Journal, 43, 179-189, 2009.

Mäki M., Aalto J., Hellén H., Pihlatie M. and Bäck J.; Interannual and seasonal Dynamics of Volatile Organic Compound Fluxes From the Boreal Forest Floor. Frontiers in Plant Science, 10, 191, DOI: 10.3389/fpls.2019.00191, 2019.

Nölscher, A. C., Williams, J., Sinha, V., Custer, T., Song, W., Johnson, A. M., Axinte, R., Bozem, H., Fischer, H., Pouvesle, N., Phillips, G., Crowley, J. N., Rantala, P., Rinne, J., Kulmala, M., Gonzales, D., Valverde-Canossa, J., Vogel, A., Hoffmann, T., Ouwersloot, H. G., Vilà-Guerau de Arellano, J., and Lelieveld, J.: Summertime total OH reactivity measurements from boreal forest during HUMPPA-COPEC 2010, Atmos. Chem. Phys., 12, 8257–8270, doi:10.5194/acp-12-8257-2012, 2012.

Nölscher, A. C., Bourtsoukidis, E., Bonn, B., Kesselmeier, J., Lelieveld, J., and Williams, J.: Seasonal measurements of total OH reactivity emission rates from Norway spruce in 2011, Biogeosciences, 10, 4241–4257, doi:10.5194/bg-10-4241-2013, 2013.

Petterson, M.: Stress related emissions of Norway spruce plants, Licentiate thesis, KTH Royal Institute of technology, Stockholm, ISBN-13: 978-91-7178-644-9, 2007.

Pinto-Zevallos, D., Hellén, H., Hakola, H., van Nouhuys, S., and Holopainen, J.: Herbivore-induced volatile organic compounds emitted by food plants of the Glanville Fritillary, Phytochem. Lett., 6, 653–656, 2013.

Praplan, A. P., Tykkä, T., Chen, D., Boy, M., Taipale, D., Vakkari, V., Zhou, P., Petäjä, T., and Hellén, H.: Long-term total OH reactivity measurements in a boreal forest, Atmos. Chem. Phys., 19, 14431–14453, https://doi.org/10.5194/acp-19-14431-2019, 2019.

Praplan, A. P., Tykkä, T., Schallhart, S., Tarvainen, V., Bäck, J., and Hellén, H.: OH reactivity from the emissions of different tree species: investigating the missing reactivity in a boreal forest, Biogeosciences, 17, 4681–4705, https://doi.org/10.5194/bg-17-4681-2020, 2020.

Possanzini, M., Di Palo, V., Brancaleoni, E., Frattoni, M., and Ciccioli, P.: A train of carbon and DNPH-coated catridges for the determination of carbonyls from C1 to C12 in air and emission samples, Atmos. Environ., 34, 5311-2318, 2000.

Rinne J., Taipale R., Markkanen T., Ruuskanen T., Hellén H., Kajos M., Vesala T., and Kulmala M., 2007. Hydrocarbon fluxes above a Scots pine forest canopy: Measurements and modeling. Atmospheric Chemistry and Physics, 7, 3361–3372.

Rinne J., Bäck J. and Hakola H.: Biogenic volatile organic compound emissions from Eurasian taiga: current knowledge and future directions. Boreal Env. Res. 14: 807–826, 2009.

Ruuskanen T., Kajos M., Hellén H., Hakola H., Tarvainen V. And Rinne J., 2007. Volatile organic compounds emissions for Siperian Larch. Atmospheric Environment. 41,5807-5812.

Räsänen J.V., Leskinen J.T.T., Holopainen T., Joutsensaari J., Pasanen P. and Kivimäenpää M.: Titanium dioxide (TiO2) fine particle capture and BVOC emissions of Betula pendula and Betula pubescens at different wind speeds. Atmospheric Environment, 152, 345-353, 2017.

Schallhart, S., Rantala, P., Kajos, M. K., Aalto, J., Mammarella, I., Ruuskanen, T. M., and Kulmala, M.: Temporal variation of VOC fluxes measured with PTR-TOF above a boreal forest, Atmos. Chem. Phys., 18, 815–832, https://doi.org/10.5194/acp-18-815-2018, 2018.

Schiestl-Aalto, P., Kulmala, L., Mäkinen, H., Nikinmaa, E., and Mäkelä, A.: CASSIA - a dynamic model for predicting intra-annual sink demand and interannual growth variation in Scots pine, New Phytol., 206, 647-659, https://doi.org/10.1111/nph.13275, 2015.

Stark, S., Julkunen-Tiitto, R., Holappa, E., Mikkola, K., and Nikula, A.: Concentrations of foliar quercetin in natural populations of white birch (Betula pubescens) increase with latitude. J. Chem. Ecol. 34(11): 1382–1391. doi: 10.1007/s10886-008-9554-8. PMID:18946705, 2008.

Tarvainen V., Hakola H., Hellén H., Bäck J., Hari P. and Kulmala M., 2005. Temperature and light dependence of the VOC emissions of Scots pine. Atmospheric Chemistry and Physics, 5, 1-10.

Vickers, C. E., Gershenzon, J., Lerdau, M. T., and Loreto, F.: A unified mechanism of action for volatile isoprenoids in plant abiotic stress, Nat. Chem. Biol., 5, 283–291, 2009.

Vuorinen T., Nerg A.-M., Vapaavuori E. and Holopainen J.K.: Emission of volatile organic compounds from two silver birch (Betula pendula Roth) clones grown under ambient and elevated CO2 and different O3 concentrations. Atmospheric Environment, 39, 1185-1197, 2005.

Vuorinen T., Nerg A.-M.m Syrjälä L., Peltonen P. and Holopainen J.K.: Epirrita autumnata induced VOC emission of silver birch differ from emission induced by leaf fungal pathogen. Arthropod-Plant Interactions, 1, 159–165, DOI 10.1007/s11829-007-9013-4, 2007.

Wildt, J., Kobel, K., Schuh-Thomas, G., and Heiden, A. C.: Emissions of oxygenated volatile organic compounds from plants, part II: Emissions of saturated aldehydes, J. Atmos. Chem., 45, 173– 196, 2003.

Yaman B., Aydin Y. M., Koca H., Dasdemir O., Kara M., Altiok H., Dumanoglu Y., Bayram A. tolunay D., Odabasi M. and Elbir T.: Biogenic Volatile Organic Compound (BVOC) Emissions from Various Endemic Tree Species in Turkey. Aerosol and Air Quality Research, 15, 341-356, doi: 10.4209/aaqr.2014.04.0082, 2015.

Yanez-Serrano A.M., Fasbender L., Kreuzwieser J., Dubbert D., Haberstroh S., Lobo-Do-vale R., Caldeira M.C:, and Werner C.: Volatile diterpene emission by two Mediterranean Cistaceae shrubs. Scientific reports, 8, 6855-6868, DOI:10.1038/s41598-018-25056-w, 2018.

Yang, Y., Shao, M., Wang, X., Nölscher, A. C., Kessel, S., Guenther, A., and Williams, J.: Towards a quantitative understanding of total OH reactivity: A review, Atmospheric Environment, 134, 147-161, https://doi.org/10.1016/j.atmosenv.2016.03.010, 2016.

840 Zhang Q.-H., Birgersson G., Zhu J., Löfstedt C., Löfqvist, J. and Schlyter F.: Leaf volatiles from nonhost deciduous trees: variation by tree species, season, and temperature, and electrophysiological activity in Ips typographus. *Journal of Chemical Ecology,* 25**,** 1923-1943, 1999.

845

850

855

860

865

870

875

880

885

890

895

Table A1. Mean emission rates (ng g_{dw}^{-1} h^{-1}) of downy birches measured with GC-MS1 together with temperature (T), relative humidity (RH) and photosynthetic radiation (PAR) on the branch chamber during the measurements in 2017 and 2019. N= number of samples. Mean afternoon maximas for total MT, OMT, SQT and OSQT and for T and PAR are shown in parenthesis.

ng g_{dw}^{-1} h^{-1}	2017			2019			
	Early	Main	Late	Bud	Early	Main	Late
N	43	249	114	179	319	434	209
T (ºC)	12	14	10	9	16	19	17
				(19)	(27)	(35)	(28)
RH (%)	19	28	43	44	82	66	63
PAR (µmol m^{-2} s^{-1})	186	144	68	n.a.	220	164	131
					(497)	(897)	(726)
isoprene	0	0	0	0	0	0	0
2-methyl-3-buten-1-ol	0	0	0	0	1	1	0
cis-3-hexenol	n.a.	n.a.	n.a.	0	0	0	6
α-pinene	58	1	32	2	15	3	2
camphene	0	0	1	0	0	0	0
β-pinene	0	0	2	0	16	5	1
3Δ-carene	4	0	24	0	1	0	0
p-cymene	2	0	0	0	1	0	0
limonene	20	2	1	0	17	3	1
terpinolene	9	0	2	0	10	2	1
myrcene	6	1	1	0	6	2	3
sabinene*	n.a.	n.a.	n.a.	0	19	3	0
β-phellandrene*	2	0	1	0	n.a.	n.a.	n.a.
4Δ-Carene*		n.a.	n.a.	0	5	0	0
β-ocimene*	n.a.	n.a.	n.a.	0	0	0	57
SUM MTs	**129**	**15**	**64**	**2**	**88**	**17**	**64**
				(12)	**(368)**	**(125)**	**(380)**
1,8-cineol	0	1	0	0	10	3	0
linalool	28	10	0	0	23	1	0
α-terpineol	1	0	0	n.a.	n.a.	n.a.	n.a.
cis-linalool oxide	n.d	n.a.	n.a.	0	6	0	0
SUM OMTs	**29**	**11**	**0**	**0**	**39**	**4**	**1**
				(0)	**(217)**	**(32)**	**(8)**
longicyclene	161	0	0	0	1	0	0
iso-longifolene	0	0	0	0	0	0	0
β-farnesene	2	4	1	53	91	33	7
β-caryophyllene	209	14	0	47	297	4	1
α-humulene	101	2	0	7	77	1	0
α-farnesene	37	117	3	0	n.a.	n.a.	n.a.
SQT1	150	2	0	0	0	0	0
SQT2	3	0	0	0	3	0	0
SQT3	5	0	0	0	1	0	0
SQT4	1	0	0	0	29	1	0

SQT5	11	0	0	0	2	1	1
SQT6	1	0	0	0	0	0	5
SQT7	9	86	1	0	n.a.	n.a.	n.a.
SUM SQTs	**692**	**226**	**5**	**108 (662)**	**505 (2359)**	**41 (316)**	**14 (108)**
caryophyllene oxide	n.a.	n.a.	n.a.	0	54	5	1
OSQT1	n.a.	n.a.	n.a.	0	13	3	0
OSQT2	n.a.	n.a.	n.a.	0	20	0	0
6-hydroxy-β-caryophyllene*	n.a.	n.a.	n.a.	0	174	22	10
OSQT4	n.a.	n.a.	n.a.	0	30	2	1
OSQT5	n.a.	n.a.	n.a.	0	32	5	3
OSQT6	n.a.	n.a.	n.a.	0	29	6	1
OSQT7	n.a.	n.a.	n.a.	0	3	0	0
OSQT8	n.a.	n.a.	n.a.	0	18	8	0
14-hydroxy-β-caryophyllene acetate*	n.a.	n.a.	n.a.	47	272	82	31
SUM OSQTs	**n.a.**	**n.a.**	**n.a.**	**47 (284)**	**651 (2672)**	**134 (623)**	**46 (339)**
pentanal	1	1	1	n.a.	n.a.	n.a.	n.a.
hexanal	5	4	6	n.a.	n.a.	n.a.	n.a.
heptanal	2	1	2	n.a.	n.a.	n.a.	n.a.
octanal	1	1	3	n.a.	n.a.	n.a.	n.a.
nonanal	0	6	10	n.a.	n.a.	n.a.	n.a.
decanal	23	3	2	n.a.	n.a.	n.a.	n.a.
ALDs	**33**	**16**	**23**	**n.a.**	**n.a.**	**n.a.**	**n.a.**

* Tentatively identified, n.a.=not available

905

910

915

920

925

930

Appendix B: Typical chromatograms
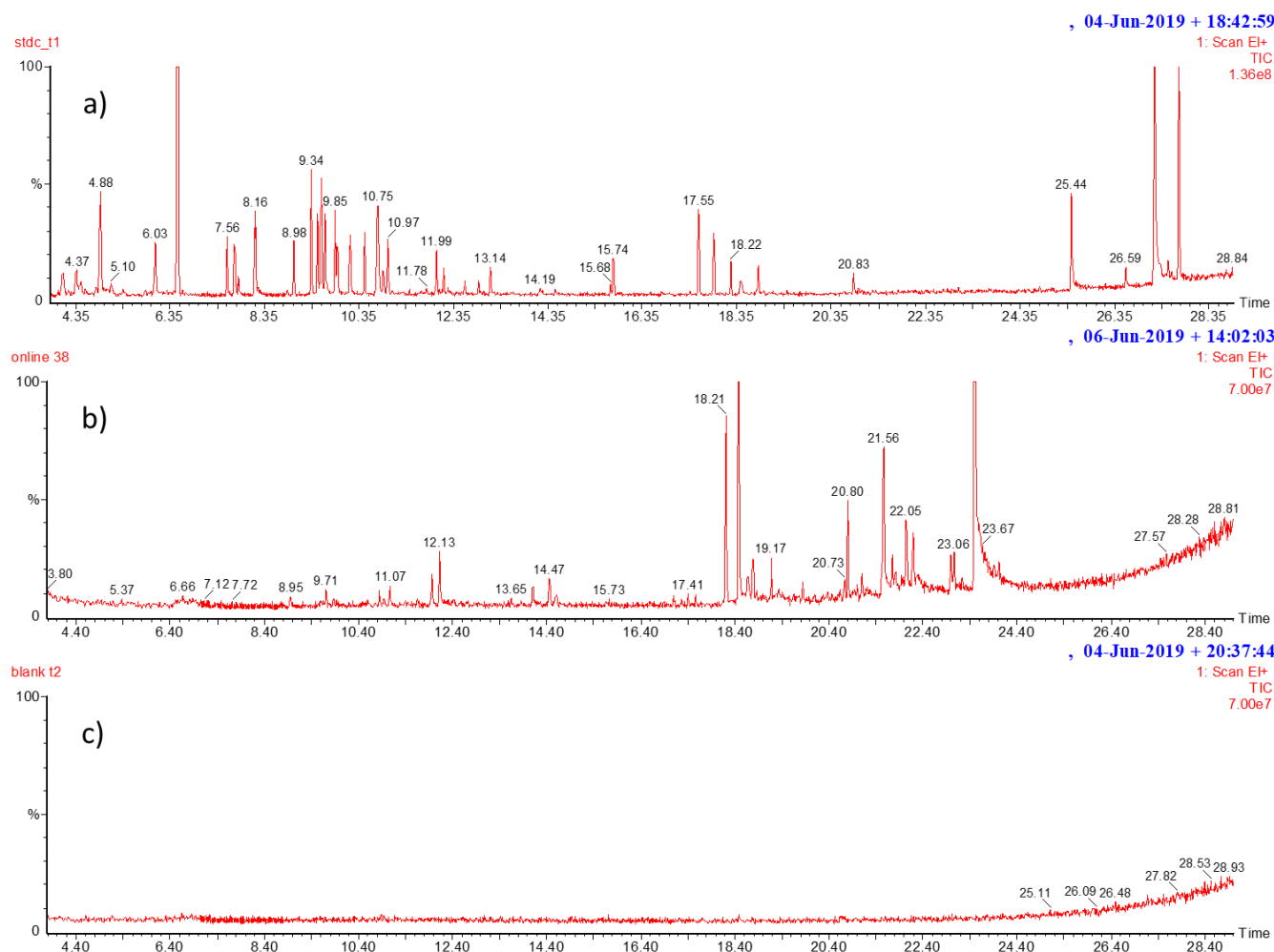
Figure B1. Examples of the scan mode chromatograms of a) calibration standard, b) birch emissions and c) blank. Peaks with corresponding retention times are isoprene (4.0), 2-methyl-3-buten-1-ol (4.56), α-pinene (8.96), camphene (9.38), sabinene (9.58), β-pinene, (9.88), myrcene (9.94), 3Δ-carene (10.46), p-cymene (10.76), limonene (10.87), 1,8-cineol (10.95), 4Δ-carene (11.10), terpinolene (11.99), cis-linalool oxide (12.13), linalool (12.239), bornylacetate (15.744), SQT1 (17.11), SQT2 (17.42), SQT3 (17.53), longicyclene (17.545), iso-longifolene (17.87), β-caryophyllene (18.235), β-farnesene (18.44), α-humulene (18.82), SQT4 (19.09), SQT5 (20.00), OSQT1 (20.65), caryophyllene oxide (20.82), OSQT1 (21.05), OSQT3 (21.44), OSQT4 (21.79), OSQT5 (22.09), OSQT6 (22.22), OSQT7 (23.03), OSQT8 (23.09), OSQT9 (23.62), cembrene (25.45), Ent-kaurene (27.195), 3-methylene-andrsastene (27.71). The calibration standard chromatogram contains multiple peaks that were anthropogenic VOCs included deliberately in the standard solution, but these were not studied in the branch emissions.

935

940

945

950

955

Appendix C: Additional birch branches

960
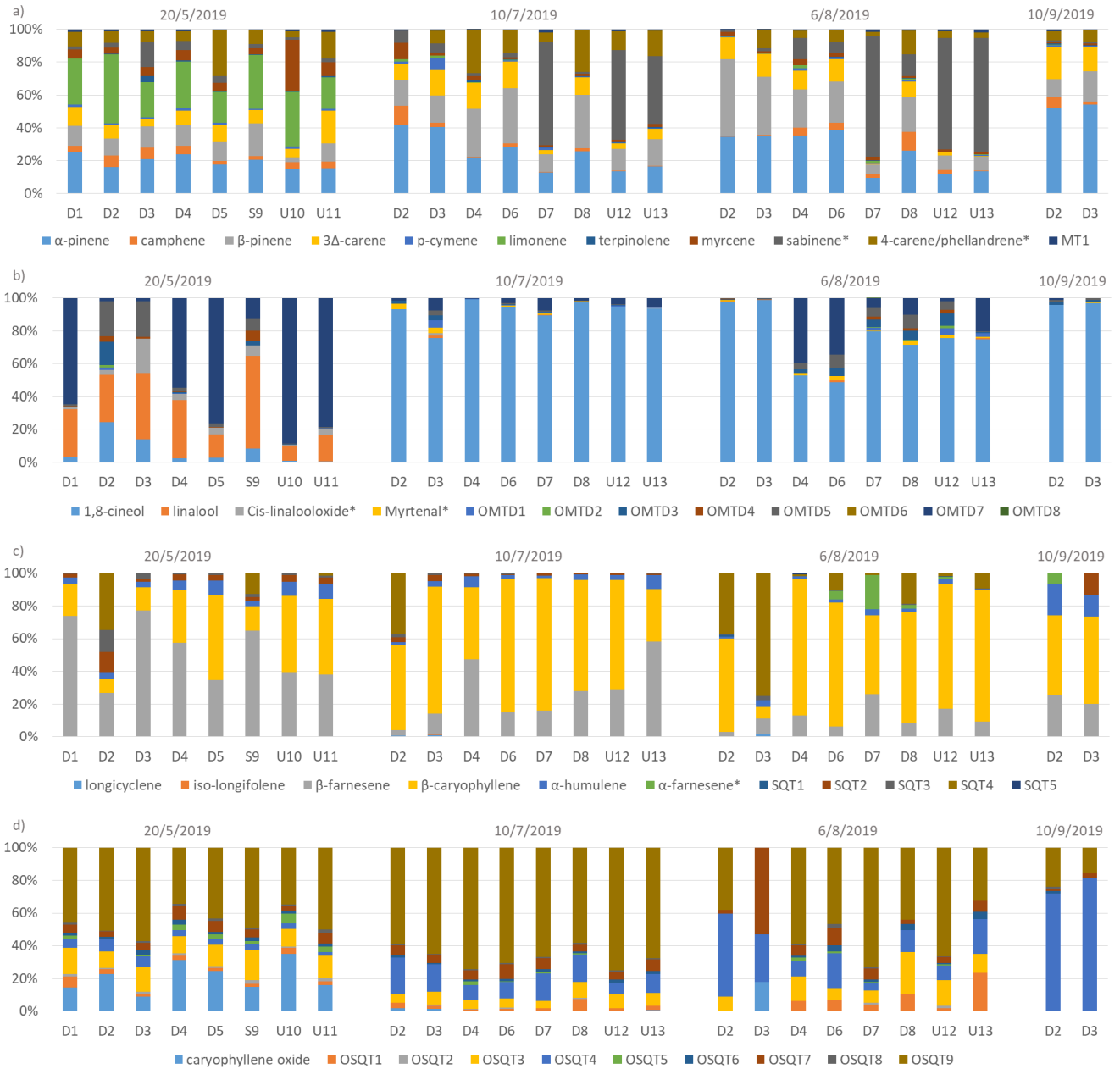
965

Figure C1. Ratios of a) MTs, b) OMTs, c) SQTs and d) OSQTs in the head space of 13 different birch branches measured over the growing season in 2019. Of the trees D1-D8 were identified as downy birches, S9 was a silver birch and U10-13 were either downy or silver birches.

970

975